Environment Canada
Environmental Protection Service

Environnement Canada
Service de la protection de l'environnement

Investigation of the Operating Parameters of the Oil Spill Containment and Recovery (OSCAR) Vessel

Technology Development
Report EPS 4-EC-81-5

Environmental Impact Control Directorate
December 1981

ENVIRONMENTAL PROTECTION SERVICE REPORT SERIES

Technology Development Reports describe technical apparatus and procedures, and results of laboratory, pilot plant, demonstration or equipment evaluation studies. They provide a central source of information on the development and demonstration activities of the Environmental Protection Service.

Other categories in the EPS series include such groups as Regulations, Codes, and Protocols; Policy and Planning; Economic and Technical Review; Surveillance; Training Manuals; Briefs and Submission to Public Inquiries; and, Environmental Impact and Assessment.

Inquiries pertaining to Environmental Protection Service Reports should be directed to the Environmental Protection Service, Department of the Environment, Ottawa, Ontario, Canada, K1A 1C8.

RE ENVIRONMENT CANADA REPORT EPS 4-EC-81-5 ENTITLED ***"INVESTIGATION OF THE OPERATING PARAMETERS OF THE OIL SPILL CONTAINMENT AND RECOVERY (OSCAR) VESSEL"***:

"The Environment Canada report EPS 4-EC-81-5 describing testing of a model contra-rotating-drum skimmer performed by Western Canada Hydraulics Ltd. in 1979 does not cover the full range of testing parameters recommended in the 1993 American Society for Testing & Materials (ASTM) oil spill skimmer testing guidelines. More recent testing, which also does not follow ASTM Guidelines, has been carried out on a commercial contra-rotating-drum skimmer in Japan in 1993. These tests, however, cover a different range of oil thicknesses, oil viscosities and operating parameters. Copies of the more recent tests can be requested from OSR Systems Ltd., 204-1001 Cloverdale Avenue, Victoria, British Columbia V8X 4C9."

INVESTIGATION OF THE OPERATING PARAMETERS OF THE OIL SPILL CONTAINMENT AND RECOVERY (OSCAR) VESSEL

by

Western Canada Hydraulic Laboratories Ltd.

for the

Environmental Emergency Branch
Environmental Impact Control Directorate
Environmental Protection Service
Environment Canada

EPS 4-EC-81-5
December 1981

Cat. No. En 46-4/81-5E
ISBN 0-662-11843-X

ABSTRACT

A study involving both experimental and analytical investigations was carried out on two contra-rotating drums as a means to recover spilled oil. The recovery process was originally postulated to be a combination of two mechanisms:

1. the pumping of oil and water up between the contra-rotating drums; and
2. oleophilic adhesion of oil to the drums.

A test facility involving two contra-rotating drums of 2.44 m diameter was established in front of a 5 m long viewing window in a laboratory flume. Currents were generated in the flume to represent towing speeds. Drum operation at varying speeds and depths of submergence was studied using light diesel oil and a heavier mixture of bunker "C" and diesel oils. Drum recovery processes were observed and recovery rates measured.

The test results showed that the pumping action played no discernible part in the recovery process.

An elementary mathematical model was developed for the oleophilic recovery process; this allowed for prediction of recovery rates of the light diesel fuel to within 16 percent of the experimentally determined values at low drum speeds. From the model and experimental results, guidelines were drawn for the optimum operation of an existing oil spill containment and recovery (OSCAR) device using contra-rotating drums. Further mathematical investigation into the oleophilic recovery process has been recommended to establish optimum drum sizes and operating parameters for future oleophilic drum recovery devices.

RÉSUMÉ

Cette étude, fondée sur des recherches expérimentales et analytiques, porte sur deux tambours tournant en sens inverse l'un par rapport à l'autre, et qui sont destinés à la récupération des hydrocarbures déversés accidentellement. Le processus de récupération devait à l'origine être basé sur une combinaison de deux mécanismes:

1. pompage des hydrocarbures et de l'eau entre les tambours; et
2. adhérence oléophile des hydrocarbures aux tambours.

Une installation d'essai comportant deux tambours tournant en sens opposés, de 2,44 m de diamètre chacun, a été montée devant une fenêtre d'observation de 5 m de long dans un canal de laboratoire. Des courants ont été induits dans le canal pour simuler le déplacement du bâtiment remorqué. On a étudié le rendement des tambours à différentes vitesses et différentes profondeurs d'immersion pour récupérer des nappes de combustible diesel léger et d'un mélange plus lourd de combustible de soute "C" et de diesel. On a observé le processus de récupération et mesuré le taux de récupération.

Les résultats des essais montrent que le pompage joue un rôle négligeable dans la récupération.

Un modèle mathématique élémentaire a été mis au point pour la récupération par substance oléophile; il a permis de prévoir des taux de récupération du combustible diesel léger voisins, à 16 p. cent près, des valeurs mesurées expérimentalement à des vitesses faibles de rotation des tambours. Des résultats de la modélisation et des expériences, on a tiré des lignes directrices en vue d'obtenir un rendement optimal d'un appareil de confinement et de récupération des déversements d'hydrocarbures (OSCAR) existant, qui comporte deux tambours tournant en sens opposés. Il a été recommandé de procéder à une étude mathématique plus poussée du processus de récupération par substance oléophile afin d'établir les dimensions et les paramètres de fonctionnement optimaux des tambours des futurs appareils de récupération par substance oléophile équipés d'un tel système.

FOREWORD

The results of a study concerning the operating parameters of the Oil Spill Containment and Recovery (OSCAR) vessel, are outlined in this report. The work was executed by Western Canada Hydraulic Laboratories Ltd. of Port Coquitlam, British Columbia, under contract to the Environmental Protection Service.

ACKNOWLEDGEMENTS

Captain D. Sjoquist of Seaspan International Ltd. has provided data and observations from previous oil spill cleanup operations during the course of this study. His assistance in doing this and in arranging a viewing of the prototype device was greatly appreciated.

Many thanks also to Mr. L. Solsberg of the Environmental Emergency Branch in Ottawa, for his advice as Scientific Authority for this project.

TABLE OF CONTENTS

LIST OF FIGURES

LIST OF TABLES

CONCLUSIONS AND RECOMMENDATIONS

CONCLUSIONS

The principal limitations on operating performance of the prototype OSCAR determined by this study are:

1. Smooth contra-rotating drums do not pump oil above the water surface for collection. They collect oil through the oleophilic attraction of the steel drums.
2. Oil is only picked up by the drum at the upstream fluid surface. The thickness of oil film developed on the drum is determined by the oil layer thickness on the water, by oil properties, and by the drum surface speed. The oil film thickness increases with an increasing drum surface speed.
3. High drum speeds and/or deep submergence lead to emulsification of the collected oil in the water underneath the drums; consequently, the thickness of the oil layer recovered by the drum is reduced.
4. The rear contra-rotating drum plays no significant part in the oil recovery process while the vessel advances through the water. Both drums pick up oil at equal rates when the vessel is stationary.
5. Emulsification of oil in water as it is carried under the drum occurs when the water boundary layer Reynolds number exceeds 5×10^5.
6. The gap width between contra-rotating drums is not a critical factor in the recovery process if there is no contact between the oil and water layers on each drum.
7. The submergence of the 2.44 m diameter prototype OSCAR drums should be set at a minimum level in order to reduce the effects of wave action.
8. The prototype OSCAR drums should be rotated at or below 5 rpm when operating in thin oil slicks or with a drum submergence greater than 30 cm to achieve optimum collection rates and a minimum entrainment of oil in water passing under the drums.
9. The optimum drum speed for the prototype OSCAR when operating in slicks of light diesel fuel more than 1.0 cm thick and with no wave action may be as high as 30 rpm. At this speed, the drums should have a submergence of less than 4 cm to minimize emulsification.
10. The vessel pushing speed should be suited to the thickness of the spilled oil, such that a localized layer build up in front of the drums will be maintained and the drum recovery rate satisfied.

11. A mathematical model of oil and water boundary layer formation around a rotating drum can be prepared to predict variations in oleophilic pickup rates in relation to drum size, operating speed and oil viscosity, provided that drum rotation is sufficiently low so that the Reynolds number of the water boundary layer is less than 5×10^5.
12. The mathematical model derived during this study for diesel fuel recovery at low drum speeds gave a recovery rate within 16 percent of that actually collected by the test facility.

RECOMMENDATIONS

The following recommendations are made on the basis of the study results:

1. Further analytical investigation into the oleophilic drum recovery processs should be carried out and a mathematical model should be prepared to accurately evaluate the effects of drum size and operating parameters on oil recovery.
2. Laboratory studies should be conducted to establish the strengths of interfacial tension between oil and steel as well as the internal cohesive forces in oils likely to be encountered in normal OSCAR operations.
3. An investigation should be made into improving the performance of the prototype OSCAR. This examination could include pumping the emulsion collected between the drums into the storage hulls or designing an oleophilic matting between the drums. The latter would scrape the water boundary layer from the rearward drum and "wick" the emulsified oil captured between the drums onto the rearward drum.

1 INTRODUCTION

1.1 Design of Prototype Machine

An unpowered, double-ended Oil Spill Containment and Recovery (OSCAR) vessel was designed by Capt. J. Steel & Co. of Victoria in 1972 and constructed by the Gulf of Georgia Towing Co. Ltd. under a grant from the Federal Department of Supply and Services.

The "catamaran-type" vessel has two identical 3.05 m long by 2.44 m diameter contra-rotating steel drums mounted laterally between the hulls (see Figure 1). The drums, which are powered by hydraulic motors, rotate towards each other at the bottom so that oil from the sea surface is collected between them. The design allows for the oil to be lifted up by the drums, scraped off and then conveyed by gravity into the twin hulls for storage. The storage hulls each house two valves incorporated into the bottom, allowing any free water which has been collected with the oil to separate out and return to the sea by gravitational flow. The vessel has been designed to collect all surface fluid, and with the separation process taking place in the storage hulls, the necessity for selective oil recovery at the water surface is eliminated. The drums are claimed to pick up 100 percent of spilled oil if left to operate for a sufficient length of time.

The designer claims that operation of the drums is not hindered by floating debris or by moderate wave action. The collection process is considered to work on all grades of spilled oils. Seaspan International Ltd. has reported a recovery rate of approximately 22.5 litres/min of light marine diesel fuel from a spill in the Port of Vancouver. The vessel has also been reported to have recovered Bunker "C" fuel from Burrard Inlet. Patent rights on the operating principle have been applied for by Petro Clearance Ltd. of Hamilton, Bermuda.

Environmental Protection Service (EPS) personnel witnessed preliminary tests of OSCAR in 1974. The design concept appeared promising and further studies were considered warranted to examine its operating principle and to evaluate its performance against other oil spill recovery vessels. The results of the preliminary tests were reported on, along with comparative tests of six other generic types of oil recovery vessels (Solsberg et al., 1976). Recommendations were made that further testing be carried out on the oleophilic drum concept to more fully examine its operating principle and to optimize its operating parameters.

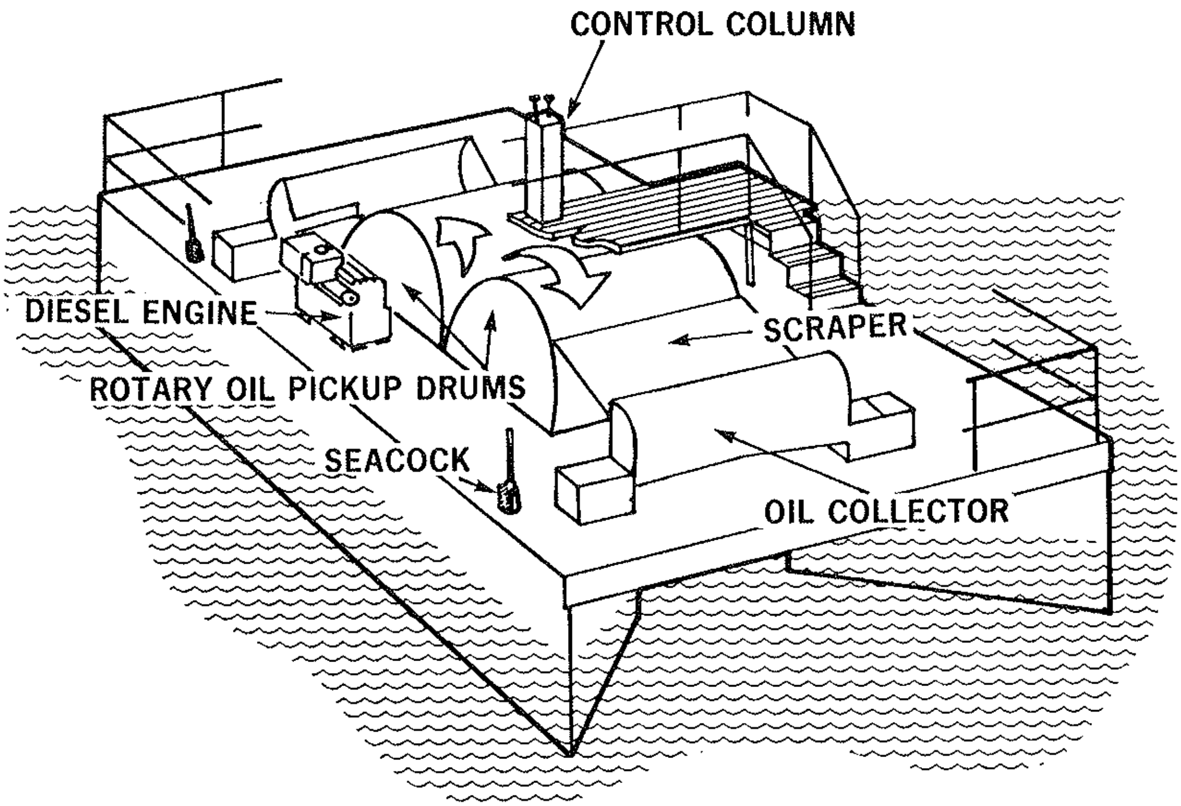

FIGURE 1 PROTOTYPE VESSEL

The purpose, then, of this study was to investigate the operating principles governing oil collection using two contra-rotating drums and to establish the relative effects of oil pumping and oleophilic attraction in the recovery process. The study was specifically designed to assess the effect of varying (1) the rotational speed of the drums, (2) the gap distance between the drums, (3) the immersion depth of the drums, and (4) the vessel speed on the oil collection rate of various oil types and slick thicknesses.

1.2 Hypothetical Operating Principles

The efficiency of the OSCAR cleanup process was thought to depend on two factors:

1. oil being retrieved from the water surface through oleophilic attraction to the steel surfaces of the two drums; and
2. oil and water being pumped up between the drums as a result of the drums' close proximity and contra-rotation.

The oleophilicity, or adhesion of oil to the surface of the drums, varies with oil composition and properties; it also varies with the characteristics of the drum surface material. The thickness of an oil layer picked up from the water by the drum through either oleophilic or pumping action is a function of oil viscosity, specific weight and interfacial tension of the oil/water phases. It is also regulated by the oil supply rate, drum speed, drum radius and the angle and height through which the drum must lift the oil.

Data were collected on the relative importance of the above factors for successful operation of the unit.

2 TEST FACILITY

2.1 Scaling Laws

The fluid properties of both oil and water which have the greatest effect upon the oil pickup rate of rotating drums are:

1. interfacial tension (σ);
2. viscosity (ν); and
3. specific gravity (γ).

Relationships amongst these factors and between the forces of fluid momentum and gravitational attraction must be maintained for comparative studies of the collection process.

To accurately model the process, the following dimensionless parameters must have similar numerical values in model and prototype:

1. densimetric Froude Number,

$$F_D = \frac{V}{\left(\frac{\rho_\omega - \rho_\omega}{\rho_\omega} \; gd\right)^{0.5}}$$

relating inertial forces to the relative buoyancy of the lighter fluid;

2. Reynolds Number,

$$R_N = \frac{VD}{\nu}$$

relating inertial to viscous forces; and

3. Weber Number,

$$W = \frac{V(\rho_o L)^{0.5}}{\sigma^{0.5}}$$

relating inertial to surface tension forces where:

V = velocity

ρ_ω = density of water

ρ_o = density of oil

g = gravitational constant

d = characteristic depth, and

L = characteristic length

Comparison of the above parameters shows that the correct interrelationships amongst linear, depth and velocity scales with the various fluid properties required to reproduce an oil spill pick up operation can only be achieved at a 1:1 scale with the actual oil and water being used as the operating fluids. A full scale model of the prototype drums in the longitudinal and vertical planes, therefore, was required for the study. The model could be built to any convenient dimension in the lateral plane, as the drum collection rate per unit width would remain unchanged apart from minor end effects at the sides of the drums.

2.2 Construction of Facility

A test facility was constructed at full scale to examine the operating process of contra-rotating drums similar to those used in the Gulf of Georgia Towing Co. Ltd.'s, OSCAR. The facility was designed so that the effects of varying the drum size and operating parameters could be studied. Two 1.22 m length, 2.44 m diameter contra-rotating prototype drums were fabricated from 2.7 mm sheet steel mounted on 1.9 cm thick circular plywood templates. The drums were mounted using 4.4 cm axles onto a 7 by 1.5 m wheeled carriage. The carriage was formed using 10 by 10 cm rough timbers with aluminum channel cross supports. Drum gap width was controlled by turning a threaded rod which adjusted the position of the axle bearings on one drum. The carriage was constructed to travel with rubber wheels on steel rails atop a 29 m long flume (see Figure 2).

The drum skins were rolled and attached with machine welded joints to give a continuous, even surface (see Figure 3). Drum rotation was produced by a 1.2 kW electric motor through an adjustable variable-speed chain drive. Oil was scraped from the drums by aluminum blades, similar to those used in the prototype, and was guided to collection tanks across hinged 1.5 mm galvanized sheet steel trays. The tray hinges permitted the scrapers to lie in close contact with the drums despite any scraper wear which took place. The scrapers could be lifted off the drums when required through use of overhead turnbuckles.

A 7.5 kW variable speed electric motor at one end of the flume was connected via a winch and a continuous 1 cm diameter cable. This apparatus towed the carriage in either direction over a 23 m length of the flume. The cable was led from one end of the carriage, around the motor-driven winch and returned; suspended by overhead pulleys to the other end of the flume. Electrical leads to the drum motor were also suspended overhead and could be towed with the carriage without significant drag.

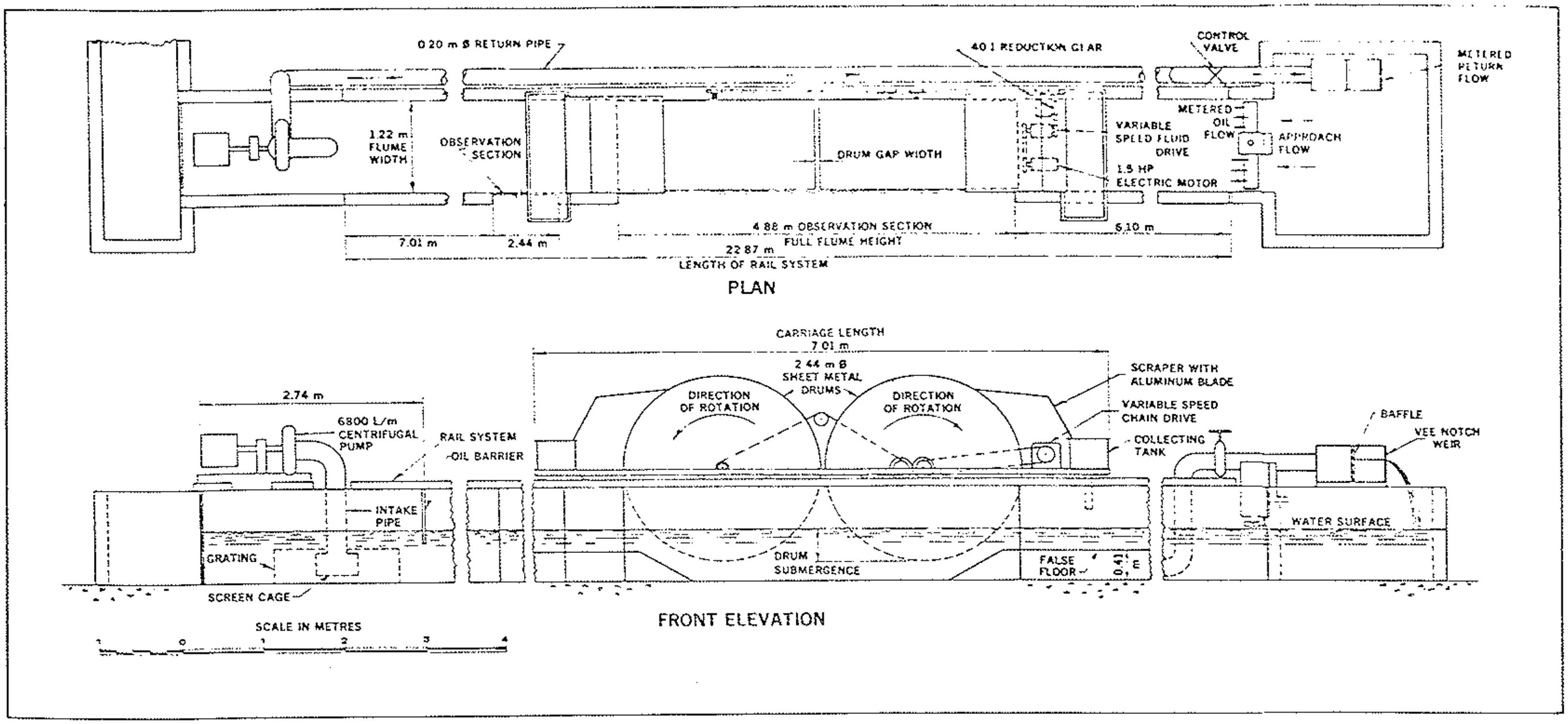

FIGURE 2 TEST FACILITY LAYOUT

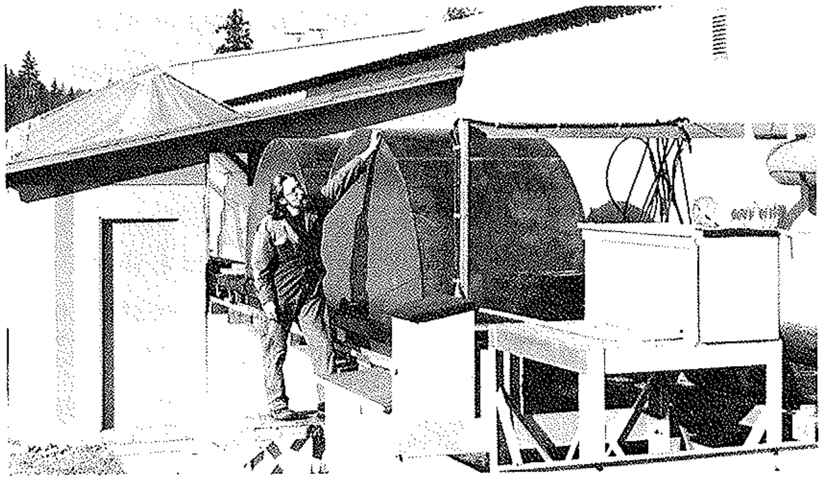

A) Drums mounted on carriage

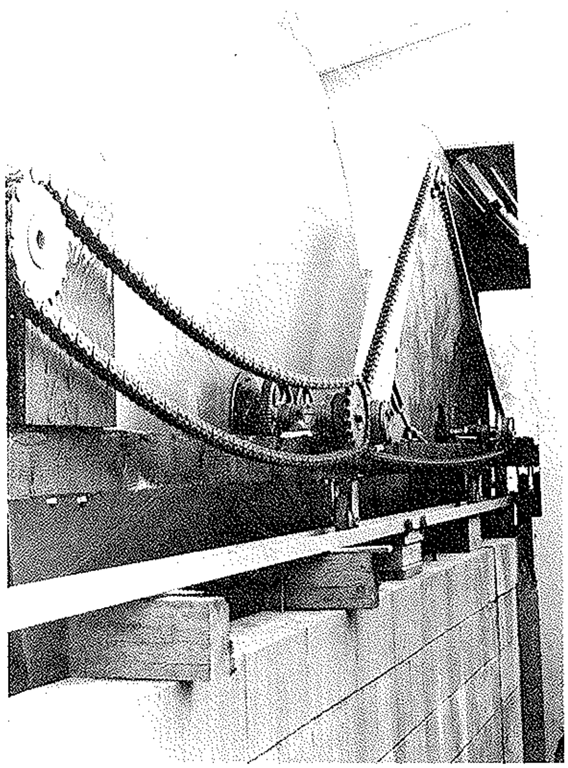

B) Chain drive for contra-rotating drums

FIGURE 3 TEST DRUMS IN FLUME

An 18 kW centrifugal pump capable of discharging 6800 L/min was installed at the downstream end of the flume to induce currents for tests in which drum operation was being studied while the carriage was stationary in front of a viewing window. A baffle wall and vortex eliminating grid cage around the pump intake prevented oil from being recirculated through the pump. The pump discharge was metred using a Vee-notch weir and controlled by a gate valve at the upstream end of the flume.

A removable 40.5 cm high flooring of galvanized sheet metal was installed both upstream and downstream of the drums to induce approximately equal flow velocities leading up to and under the drums during non-towing tests. The floor sloped in towards the drum from both sides at an angle of approximately 30°. With a depth of water in the flume of 71 cm, equivalent to a drum submergence of 30.5 cm, the flow depth over the false floor was the same as that under the drums.

A 0.4 kW pump supplied test oil from 200 L drums to an oil distribution trough constructed of galvanized steel across the upstream end of the flume. An adjustable weir was fabricated of sheet steel to maintain a constant head over a circular horizontal metering orifice in the supply system leading to the distribution trough.

3 STUDY PROGRAM

3.1 General Outline

The study program was conducted in three stages:

Stage I

Preparatory tests to determine appropriate test oils and drum surface textures.

Stage II

Flume studies to examine the operating action of the drums; to collect data for use in calibrating subsequent analytical studies.

Stage III

Analytical studies to gain a better understanding of the oil collection process and to investigate, with the aid of the data collected during Stage II, the development of a numerical predictive method for optimizing the OSCAR design and operation.

3.2 Test Program

Preparatory Tests - Stage I

The suitability of six oils was examined for use in the Stage II test program. The oils examined were:

Diesel fuel,
Royal fuel,
Oil Mix No. 54,
Essolube 30,
Fuel Oil No. 46, and
Bunker "C".

Properties of these oils are presented in Table 1 and Figure 4.

Seven test plates with different surface characteristics were examined to determine their relative effectiveness in picking up Royal fuel oil from a water surface. The plate surfaces were:

Aluminum,
Steel with light rust,
Steel with moderate rust,
Galvanized steel,
Zinc chromate paint,
Red lead paint, and
Polypropylene sheeting.

TABLE 1 PROPERTIES OF TEST OILS CONSIDERED AND WATER

Oil Type	API Gravity	Specific Gravity	Viscosity 0°C dynamic Pa.s	Viscosity 0°C kinematic cm^2/s	Viscosity 8°C dynamic Pa.s	Viscosity 8°C kinematic cm^2/s	Viscosity 15°C dynamic Pa.s	Viscosity 15°C kinematic cm^2/s	Surface Tension Beneath Air mN/m 0°C	Surface Tension Beneath Air mN/m 8°C	Surface Tension Beneath Air mN/m 15°C
Water		0.999	0.0018	0.018	0.0014	0.014	0.0011	0.011	75.60	74.58	73.56
Diesel Fuel	38.0	0.835	0.01	0.12	0.008	0.093	0.006	0.074		23 to 32	
Royal Fuel	23.0	0.916	0.098	1.07	0.068	0.744	0.06	0.651		23 to 38	
Oil Mix 54	22.8	0.917	0.16	1.74	0.098	1.07	0.074	0.807		23 to 38	
Essolube 30	27.9	0.888	1.96	22.03	0.548	5.95	0.494	5.39		33 to 54	
Fuel Oil 46	17.4	0.950	7.68	80.86	1.89	19.89	0.848	8.92		—	
Bunker "C"	13.8	0.974	—	—	—	—	—	—		—	

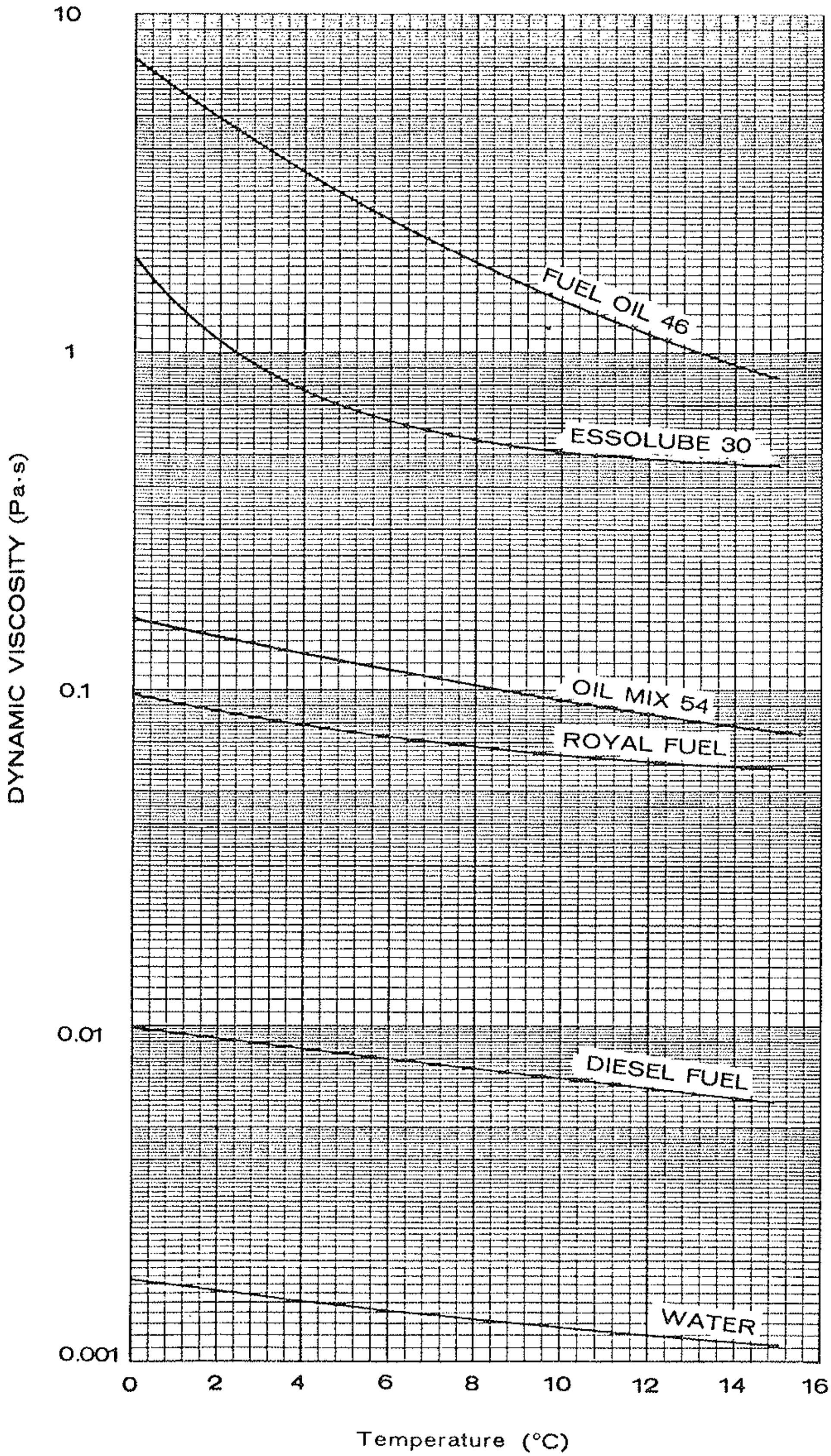

FIGURE 4 DYNAMIC VISCOSITIES OF OILS AND WATER

From these tests the drum surface and test oils to be used in the Stage II flume studies were selected.

Flume Tests - Stage II

The test program carried out in the flume is presented in Table 2. The effect on oil collection rates with two types of oil was studied. Drum speed was varied between 5 and 15 rpm at depths of submergence between 11.5 and 45.0 cm.

Following test runs with the 2.44 m diameter drum located in front of the viewing window in the flume, it was decided to forego testing using the carriage towing arrangement. Further work on the project was confined to investigation of the drum collection process through theoretical and mathematical analysis.

Analytical Studies - Stage III

A theoretical investigation was made into the basic principles of the oil pickup process. The analysis developed a boundary layer theory and was used to assess the effect of drum speed on the oil recovery rate.

TABLE 2 FLUME TEST PROGRAM

Test Series	Oil Type	Approach Velocity m/s	Drum Parameters: Rotation rpm	Drum Parameters: Submergence cm	Purpose of Series
1	Diesel	0.23	5, 10, 13	11.4	Effect of Rotation Speed
2	Diesel	0.17	5, 10, 15	30.5	Effect of Submergence
3	Diesel	0.14	5	45.0	Effect of Submergence
4	Diesel	0.00	5, 10		Effect of Approach Velocity
5	Diesel	0.00	10		Effect of Layer Thickness
6	Oil Mix 54	0.17	5, 10, 15	30.5	Effect of Oil Properties

4 TEST PROCEDURES

4.1 Preparatory Tests

Samples of six commercially available oils were obtained and analyzed for viscosity and specific gravity at temperatures down to 0°C. Two of these oils, diesel fuel and Oil Mix No. 54, a mixture of 46 percent diesel oil and 54 percent Bunker "C" oil, were selected for use in the study on the basis of viscosity, ease of handling and availability. These oils were considered to be representative of oils likely to be discharged or spilled into Burrard Inlet. They were typical of oils in which the prototype OSCAR vessel would be expected to work.

Five steel plates, each with a different coating, measuring 15 by 15 by 0.3 cm, were examined for their relative adhesion to oil. The plate surfaces tested included light rust, medium rust, galvanized, zinc chromate paint, and red lead paint, in addition to aluminum and polypropylene plates. The plates were weighed dry and then immersed to their full depth through a 2.5 cm layer of diesel fuel overlaying a water bath. They were withdrawn vertically over a period of 2 seconds and allowed to drain for 5 seconds. Then they were reweighed in a collecting tray to determine the amount of oil still adhering to each plate. The results of these tests are shown in Figure 5.

A brief test was conducted with Fuel Oil No. 46 to assess the effect of oil layer thickness on the amount picked up by the plates in the above tests. The steel plate with light rust was repeatedly dipped into the oil bath, weighed and wiped clean. The amount of oil removed each time was subtracted from that previously in the bath and the new layer thickness calculated. The results of this test are shown in Figure 6.

4.2 Flume Tests

The drum carriage was installed under cover in front of a 5 m long full height viewing window in the side of the flume. The flume was filled with water to submerge the lower portions of the drums, and the circulating pump started, generating a current along the flume and under the drums. Oil was introduced at a steady rate through the distribution trough at the upstream end of the flume and carried by the current to the drums.

Prototype operations have been run with drum speeds up to 60 rpm; however, reports of Capt. D. Sjoquist and others who have been present at such operations indicated that there was excessive splashing and spraying of oil off the drums at these speeds and

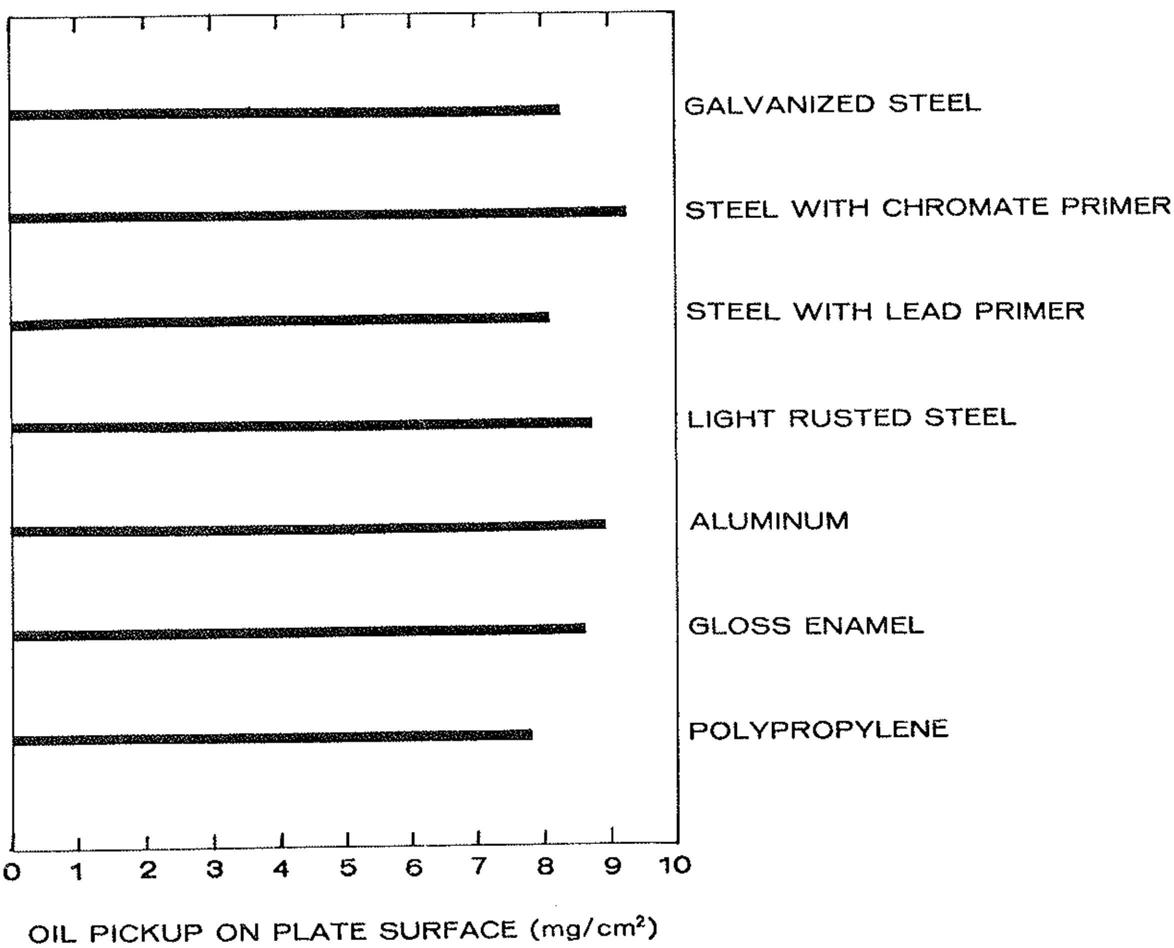

NOTE : Test plates were dipped through a 2.5 cm layer of diesel fuel.

FIGURE 5 OIL PICKUP BY VARIOUS SURFACES

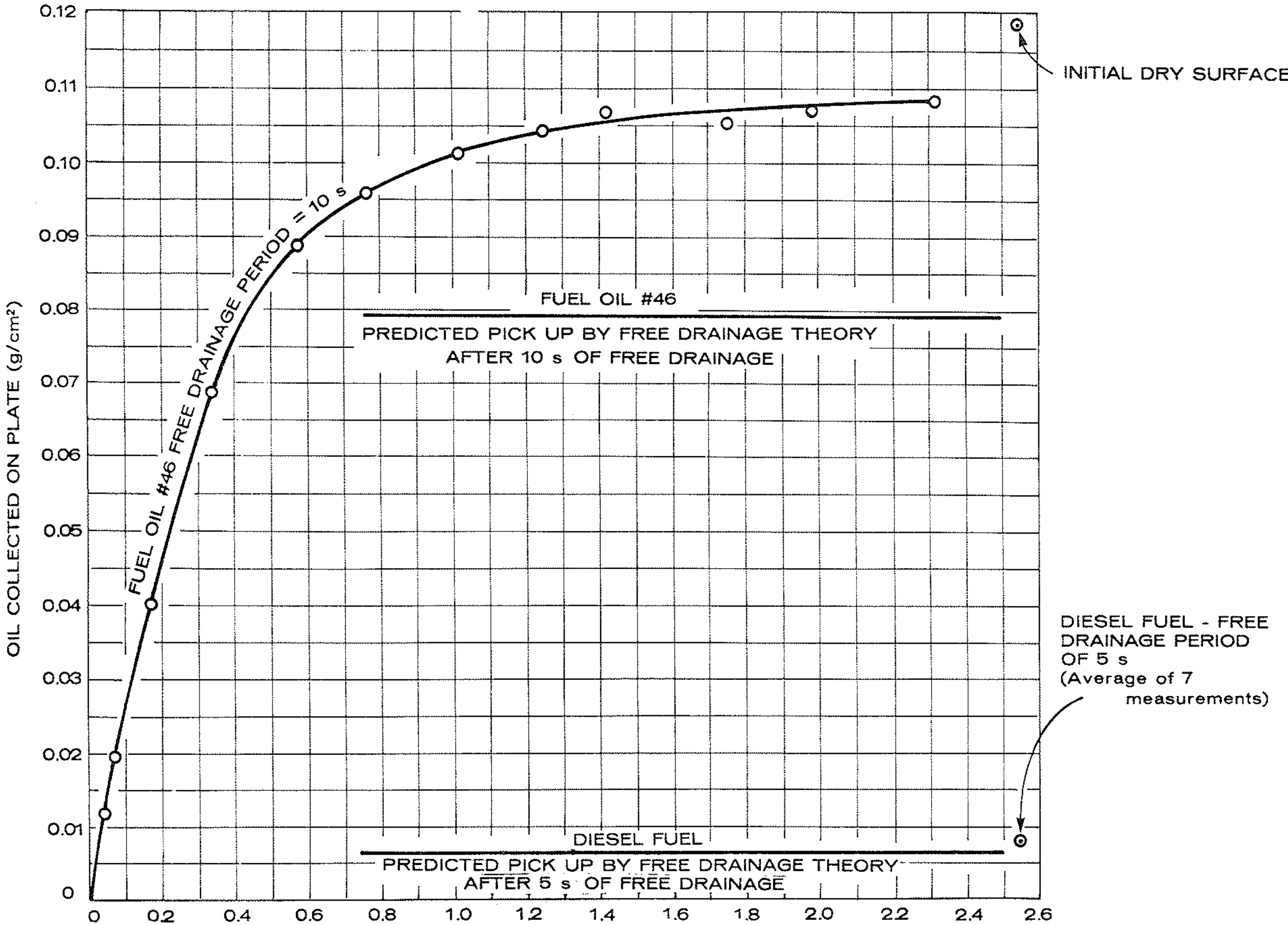

FIGURE 6 OIL PICKUP VERSUS OIL LAYER THICKNESS

that the collection system produced less oil-water emulsion at lower speeds. Model drum speeds were controlled between 5 rpm and a maximum of 15 rpm with the variable speed motor control. Power losses in the drive system prevented drum operation at speeds much in excess of 15 rpm. Drum submergences between 11.5 and 45.0 cm were examined by varying the water level in the flume.

Oil collection rates were measured by a volumetric/time method. Percentages of oil and water in the collected fluid were visually measured through a clear plastic panel in the side of the metering tank after a sample had been allowed to stand for 10 minutes. The speed of the oil layer approaching the drums was determined by timing markers over a distance of 5 m upstream of the drums. The average oil layer thickness was calculated from the oil input and current measurements. The buildup of oil layer thickness upstream of the drums was observed through the viewing window.

A black and white video tape record was made of the tests through the viewing window, illustrating the emulsification and mixing processes that occurred between the drums. A schematic diagram of the flow process is shown in Figure 7. Results of test measurements are given in Table 3 and are illustrated in Figure 8.

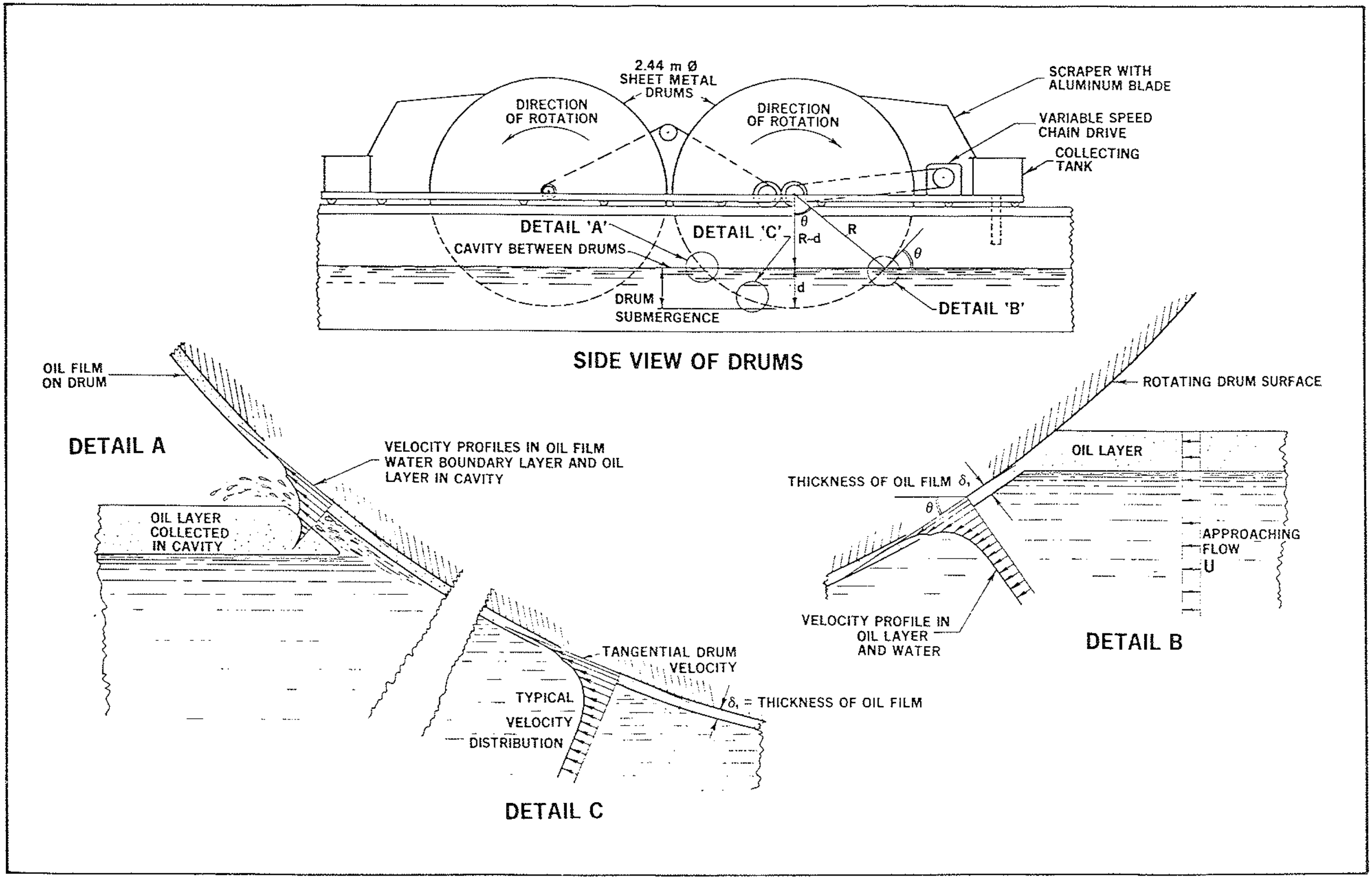

FIGURE 7 SCHEMATIC OF OIL/WATER BOUNDARY LAYER

TABLE 3 RESULTS OF FLUME TESTS

Oil Type	Drum Submergence	Gap Width	Average Approach Conditions		Drum Speed	Oil Collected		Cumulative Recovery rate	Avg. Oil Thickness on Drum	Oil Recovery Factor	Oil Content Factor
			Velocity	Oil Thickness		Upstream Drum	Downstream Drum				
	cm	cm	m/s	cm	rpm	L/min	L/min	L/min	cm	%	%
Diesel	11.4	1.2	0.23	0.3	5	12.1	0.0	12.1	0.026	23	94
	11.4	1.2	0.23	0.3	10	18.3	0.4	18.7	0.020	42	79
	11.4	1.2	0.23	0.3	13	26.4	0.5	26.9	0.022	44	66
	30.5	1.6	11.7	0.2	5	11.6	0.5	12.1	0.026	39	88
	30.5	1.6	0.17	0.3	10	23.0	0.5	23.5	0.025	79	81
	30.5	1.6	0.17	0.3	15	27.5	0.1	27.6	0.020	70	67
	45.0	1.2	0.14	0.3	5	10.6	0.0	10.6	0.023	32	94
	30.5	1.6	0.00	0.3	5	8.2	6.3	14.5	0.031		
	30.5	1.6	0.00	0.6	10	3.3	2.1	5.4	0.008		
	30.5	1.6	0.00	0.3	10	2.0	1.3	3.3	0.004		
Oil Mix 54	30.5	1.2	0.17	0.2	5	17.0	0.0	17.0	0.036	82	96
	30.5	1.2	0.17	0.2	10	18.0	0.2	18.2	0.019	93	43
	30.5	1.2	0.17	0.2	15	17.1	0.7	17.8	0.013	90	19

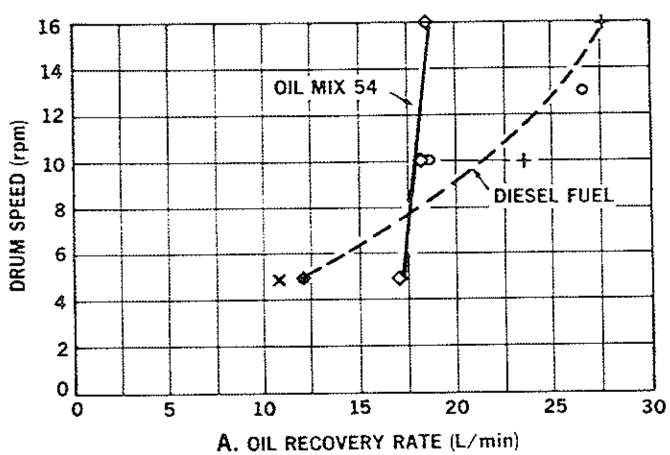

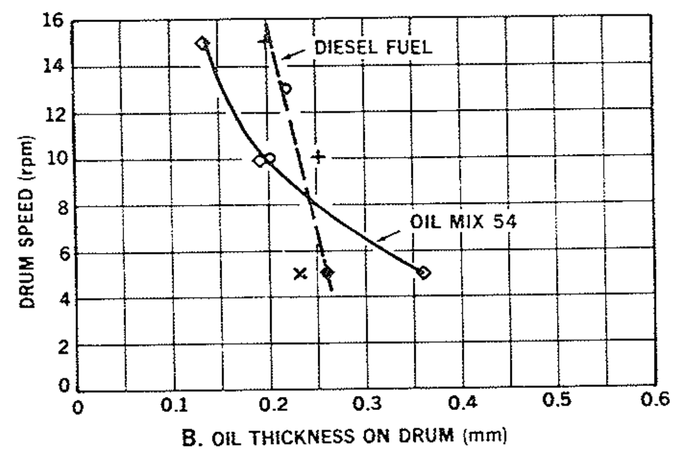

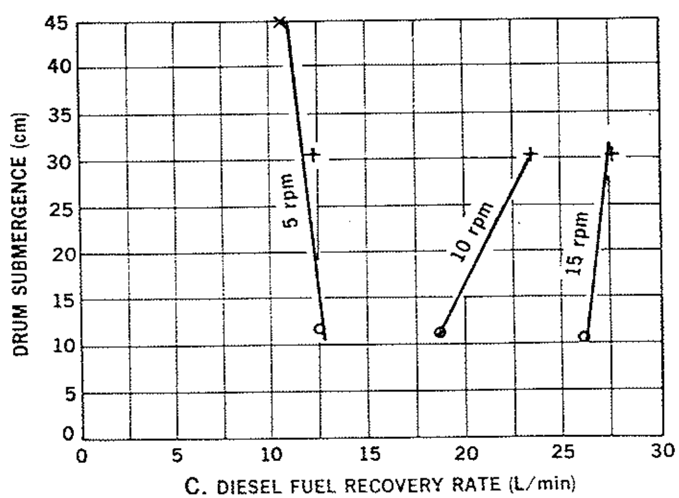

NOTE:

SYMBOL	TEST OIL	DRUM SUBMERGENCE
o	DIESEL	11.4 cm
+	DIESEL	30.5 cm
×	DIESEL	45.0 cm
◇	OIL MIX 54	30.5 cm

The test results represent the recovery process only at the rate of oil supply and layer thickness used in the tests. Measurements taken from these tests should not be used to numerically predict conditions at other oil supply rates.

FIGURE 8 EFFECTS OF VARYING OPERATING PARAMETERS

5 TEST RESULTS

5.1 Preparatory Tests

Drum Surface Material

Figure 5 illustrates that little difference exists in the oil pickup capabilities of the seven test plate surfaces. The steel plate with zinc chromate primer produced the greatest pickup of 9.1 mg/cm^2 of diesel fuel. This was approximately 12 percent more than the amount picked up by the lightly rust coated bare steel surface.

It had been found in the prototype OSCAR that a painted surface on the steel drums was scraped off during drum operation. For reasons of test simplicity and to prevent any change in surface characteristics during testing, the test drums were made of bare steel on which little rust developed due to the presence of residual oil.

Effect of Layer Thickness

Repeated test runs of lifting the bare metal test plate through a decreasing layer thickness of Fuel Oil No. 46, (Figure 6), showed that the oil pickup by the plate was approximately constant above a layer thickness of 1.2 cm. Below this layer thickness, the amount of oil pickup on each run decreased with the decreasing oil layer thickness. As the oil layer became thinner, the plate pickup capacity exceeded the local supply rate.

The test results indicate that the OSCAR's oil recovery rate of viscous oil through adhesion may decrease markedly if steps are not taken to prevent an oil slick becoming thinner in the final stages of a cleanup operation. The rate of drum rotation would not have an appreciable effect on the pickup rate under these conditions, as the drum could remove oil faster than it would flow to the drum. Figure 6 shows that the maximum oleophilic pickup rate of Fuel Oil No. 46 could not be achieved unless the oil layer thicknesses were maintained in excess of approximately 1.2 cm.

The measured pickup rates of both Fuel Oil No. 46 and diesel fuel by the steel plate were approximately 35 percent higher than those calculated from the free drainage theory (see Figure 6).

5.2 Flume Studies

Visual Observations

The clear plastic windows in the side of the flume permitted viewing of the oil collection process below the fluid surface. The flow process is depicted in Figure 8.

It was observed that the drag of the drum induced motion in the oil film and also in the surrounding water layer. The oil film was sheared off from the oil slick upstream of the first drum and was carried under the drum back to the fluid surface in the centre cavity area between the drums. The dragged water layer outside the oil film was thrust up into the cavity and it isolated the collected oil floating in the cavity from the drum surface. Emulsification occurred along the oil and water interface as drum speeds were increased to above 10 rpm. At drum speeds in excess of 10 rpm, considerable turbulence was generated in the region between the two drums with a buildup of an oil and emulsified oil layer of up to 12 cm thickness. A thin oil layer adhered to the drum and was carried around to the scraper. The drum carried the oil up to the scraper faster than it could run back down in sheet flow.

Oil was not fed to the downstream drum; therefore, only a water layer formed around the drum, which was thrust into the cavity, isolating the floating oil in the cavity from the second drum. As a result, little or no oil was picked up by the downstream drum. The second drum was relatively effective, however, in reducing the loss of oil droplets from the cavity region to the downstream region.

In tests run with zero approach velocity in the flume, the downstream drum was observed to collect approximately the same amount of oil as the upstream drum.

A return oil flow occurred between the drum and the viewing window, indicating an increase in the surface level in the cavity, over that existing upstream and downstream. The surface level difference was a result of the density difference between the water and the oil and emulsion layer in the drum cavity. A maximum difference of 0.6 cm was measured between the level in the cavity and that upstream of the drums during tests with the 10 rpm drum speed and no approach current.

Varying the gap width between the drums on the oil collection process did not have any observable effect.

Measurements from Rotating Drum Tests

The test results in Table 3 show that the downstream drum did not collect any significant amount of oil when a flume current was generated to simulate towing conditions. With zero current in the flume, the two drums collected oil at an approximately equal rate. These observations tend to confirm that the collected oil/emulsion in the cavity is isolated from the drum surfaces by the water boundary layers surrounding the drums. Only oil floating at the forward end of a rotating drum can be collected.

The test results in Figure 8 show that the oil recovery rate of diesel fuel increased with increasing drum speed while that of Oil Mix No. 54 remained relatively constant (see Figure 8a). Calculation of the average oil film thickness at the top of the drums, based on measurements of the collection rate and drum speed, shows that the thickness of the diesel fuel film decreased with increasing drum speed (see Figure 8b). This indicates that the diesel oil film thickness used in the tests was too thin to permit an adequate supply of oil to the drums. A greater supply rate than that used would have produced a thicker upstream oil layer and consequently increased the recovery rates at higher drum speeds.

As a result of its high viscosity, the Oil Mix No. 54 was introduced into the flume at too slow a rate to form a continuous oil cover on the water. The oil travelled down the flume in patches covering approximately 50 percent of the water surface. The oil supply rate was lower than the maxmium recovery rate of which the drum was capable. The decrease in oil layer thickness with increasing drum speed was more pronounced with the Oil Mix No. 54 than with the diesel but it also resulted from the low supply rate.

Diesel fuel collection rates achieved by the drums were between 10 and 28 L/min with an approach current; they were between 3 and 15 L/min when an approach current was not present in the flume. The Oil Mix No. 54 was recovered at a rate between 17 and 19 L/min. These rates compare favorably with the 9 L/min rate of light marine diesel fuel collected per 1.22 m drum length achieved by the prototype OSCAR during cleanup operations in the Port of Vancouver (1975). It is considered, however, that an increase in these recovery rates could be attained if an adequate amount of oil was available to the drums.

The oil recovery rate was not greatly affected by drum submergence (see Figure 8c). Also, there was no relationship between drum submergence and oil layer thickness at the scraper. In the presence of any pumping action that might take place, drum submergence has a greater effect on oil recovery than does oleophilic attraction of the steel drums. The results indicated, however, that pumping did NOT play a major part in the collection process.

The Oil Recovery Factor is defined as the percentage of oil collected compared to that which is available for collection during a test period. During tests in which vessel speed was simulated by a flume current, the drums picked up between 23 and 79 percent of the diesel fuel. The greatest percentage recovery was obtained with a drum submergence of 30.5 cm and an operating speed of 10 rpm. Recovery of the Oil Mix No. 54 was approximately 90 percent, with a maximum of 93 percent recorded at 10 rpm.

5.3 Effect of Drum Size

The effect of drum size on the oil recovery operation was considered on a theoretical basis. Investigation was conducted into the effect on oil recovery rates of varying the drum diameter assuming a constant drum surface velocity so that drum rotational speed varied inversely as the drum diameter.

The effect of a varying drum size on oleophilic attraction and on a possible pumping action induced in the oil and water layers surrounding the drums was considered. The oleophilic pickup rate was not considered to vary significantly with drum diameter as long as the speed at which the drum surface lifted from the water was kept constant. This theory was supported by the flume test results which had shown that submergence of the drums, and therefore the exit angle of the drums from the fluid, as well as the height to which the oil had to be lifted, had little effect on the oil recovery rate. Other factors affecting oleophilic pickup, such as adhesion of the oil to the drum, were considered unlikely to change significantly with drum surface curvature.

The relationship between drum size and the four major factors governing pumping action by the smooth drums was examined. These factors were:

1. The energy imparted to the surrounding fluid by the drum. The power absorbed by windage in turbine operations, i.e. the energy imparted by mechanical rotation to the surrounding fluid, has been found empirically to vary with $D^4.n^3$; where D is diameter and n is the speed of rotation.
2. The momentum of pumped fluid at the surface, which would vary with $D^2.n^2$.
3. The centrifugal force which would throw the fluid away from the drum and vary with $D.n^2$.
4. The air pressure differential across the fluid layer which would act to hold the fluid layer to the drum and would vary with $D^2.n^2$.

Improvement of pumping action by the drums would involve maximizing items 1, 2 and 4 above, while minimizing item 3. For a constant drum surface velocity, these could only be achieved by increasing the drum diameter, "D" and operating at lower rotational speeds, "n". It was concluded that, with any possible pumping action, operating a smaller drum at higher speeds would produce a lower recovery rate than that which was achieved with the 2.44 m diameter drum.

6 ANALYTICAL MODEL OF RECOVERY PROCESS

6.1 Important Parameters in OSCAR Process

The tests indicated that the contra-rotating drums did not produce the expected rotary pump action. They further indicated that drum submergence and spacing had relatively minor effects.

Drum speed was found to be important with respect to both the quantity and, to an even greater extent, the quality of oil collected. At higher drum speeds the oil became emulsified.

Oil viscosity was also an important factor as indicated by the relative oil film thickness on a vertical plate when it was removed from a 2.5 cm thick oil layer on water.

The plate film thickness was predicted using the withdrawal and drainage theories of Tallmadge and Gutfinger, 1976. These theories are summarized in Appendix 1. The measured pickup rates of both diesel fuel and Fuel Oil No. 46 were approximately 35% higher than those calculated from this analytical theory (see Figure 6). Also, the vertical plate tests showed that the thickness of the oil film on the plate was dependent on the oil slick thickness for relatively thin slicks. The withdrawal and drainage theories do not account for variations in oil slick thickness.

Development of a mathematical model of the oleophilic collection process was undertaken within constraints imposed by lack of published data on the physical properties of oil/water interfaces and of oil/water emulsions.

6.2 Analytical Model

Qualitative Considerations of Boundary Layer Processes

In the flume studies, both drums developed oil/water boundary layers which resulted in complete isolation of the floating oil layer in the cavity. The schematic diagram in Figure 7 illustrates the flow process near the cavity and shows that a thin oil layer coated the drum surface. Adjacent to the oil layer was a boundary layer of water which developed sufficient momentum to remove the floating oil in the cavity from the surface of the drum. Therefore, oil could not be picked up from the cavity area.

When rotational drum speeds were increased the flow became unstable due to either centrifugal instability in the oil or water boundary layer, or instability of the oil/water interface, due to formation of Kelvin-Helmholtz waves.

Criteria for centrifugal instability in viscous flows are described by Tallmadge and Gutfinger (1967). To apply these criteria, however, it is necessary to know the radial velocity profile of the boundary layer. An approximate velocity profile was obtained using a boundary layer collection model for OSCAR.

Kelvin-Helmholtz waves at an oil/water interface were discussed and described in terms of interfacial velocities and resistance coefficients by Milgram and Van Houten, (1978). They showed experimentally that interfacial waves first began to grow for interfacial velocities of approximately 25 cm/s between diesel fuel and a water surface. They also showed that the breaking of the Kelvin-Helmholtz waves at higher interfacial velocities of approximately 45 cm/s was associated with the formation of oil droplets and emulsions. Milgram and Van Houten further showed that droplet formation is maximized if the oil boundary layer is thin.

Analytical Formation of Oil Boundary Layer Process

Oil collected at the scraper of the upstream drum originates in the oil layer at the upstream surface. The film thickness is controlled by a balance between shear forces and pressure forces with either centrifugal forces and/or Kelvin-Helmholtz waves becoming important at high rotational speeds. A model which accounts for only shear, hydrostatic and pressure forces has been schematized in Figure 7. It is assumed that this model represents the test conditions up to rotational speeds before either centrifugal or Kelvin-Helmholtz instabilities develop. The model does not apply to oil collection on the downstream drum where the water boundary layer isolates oil in the cavity from the drum. The derivation of the model is presented in Appendix II.

This discharge in the oil boundary layer can be calculated only if the shear stress at the drum (τ_0) and the boundary layer thickness (σ_1) can be evaluated as a function of the distance (s) from the leading edge. On the basis of experimental results discussed by Tallmadge and Gutfinger (1967), it is expected that the oil thickness will not vary greatly with distance from the leading edge unless it is disturbed by turbulence. Moreover, its thickness can be estimated approximately by the use of the theories developed for plate withdrawal from liquid baths (see Appendix I).

6.3 Water Boundary Layer Process

Equation (4), (see Appendix II for equations 1-7) relates the shear stress in the oil at the drum surface to the stress at the oil/water interface, (τ_1). The latter can be estimated by application of the Karman integral momentum equation to a control volume which has the oil/water interface as its boundary. In this estimation of stress, it is also assumed that the velocity profiles in the water boundary layer adjacent to the oil film remain similar in the downstream direction. Derivation and application of the above equation to the water boundary layer is presented in Appendix III. From an assumed velocity profile in the water boundary layer, the required value of the shear stress (τ_i) at the oil/water interface may be determined and the oil discharge calculated using equation (6).

6.4 Range of Boundary Layer Model Application

As the boundary layer model is based on the assumption that the laminar flow is maintained in both the oil and water layers, its range of application is limited to cases where the Reynolds numbers for the oil and water layers, as defined by equation (7), do not exceed a value of approximately 5×10^5. This limits the use of the analytical model to maximum rotational speeds of between 5 and 10 rpm for a 2.44 m diameter drum with 30.5 cm submergence. Smaller drums, or drums with less submergence have a shorter wetted perimeter; hence the Reynolds number is smaller and the onset of turbulence delayed. The analytical model is therefore applicable in situations which cover a larger speed range.

High drum speeds cause the onset of turbulence as well as the occurrence of instabilities at the oil/water interface which lead to the formation of oil globules and their entrainment into the free stream flow of water. An analytical model of the latter process was not developed as part of this project.

6.5 Comparison of Predicted and Actual Recovery Rates

Recovery rates of both diesel fuel and Oil Mix No. 54 were measured for drum speeds of 5, 10 and 15 rpm at an approach current of 0.17 m/s and a drum submergence of 30.5 cm (see Table 3). Fluid properties and operating variables were selected to correspond with the above test runs. Predicted values were obtained for: the Reynolds numbers in the water boundary layer; the oil boundary layer thickness in the laminar region; and the theoretical model discharge. These were tabulated and compared with the test results, Table 4.

The Reynolds numbers of the water boundary layer in Table 4 indicate turbulence had set in at a drum speed of about 5 rpm. The test results show emulsification of both diesel fuel and Oil Mix No. 54 at a drum speed of 10 rpm. It

TABLE 4 COMPARISON OF PREDICTED AND OBSERVED RECOVERY RATES (drum submerged to 30.5 cm)

						Water Boundary Layer		Oil Boundary Layer Diesel Fuel			Oil Boundary Layer Oil Mix No. 54		
rpm	Distance from Leading Edge s_m	Angle θ degrees	Drum Surface Velocity V_t m/s	Free Stream Velocity U m/s	Effective Free Stream Velocity U_e m/s	Reynolds Number $\times 10^5$	B.L. Thickness mm	Oil Film Thickness mm	Theoretical Recovery L/min	Experimental Recovery L/min	Oil Film Thickness mm	Theoretical Recovery L/min	Experimental Recovery L/min
5	0	41.4	0.64	0.17	0.47	0	0	0.29	13.5	11.6	1.78	83.0	17.0
	0.30	27.12				1.03	5.7						
	0.60	12.8				2.06	8.1						
	0.90	-1.6				3.09	9.9						
	1.20	-15.9				4.11	11.5						
	1.50	-30.2				5.15	12.8						
	1.76	-41.4				5.95	13.8						
10	0	41.4	1.28	0.17	1.11	0	0	0.45	42.0	23.0	2.63	246.0	18.0
	0.30	27.1				2.05	4.1						
	0.60	12.8				4.12	5.7						
	0.90	-1.6				6.17							
	1.20	-15.9				8.23							
	1.50	-30.2				10.30							
	1.76	-41.4				11.90							
15	0	41.4	1.92	0.17	1.75	0	0	0.59	82.7	27.5	3.32	465.1	17.1
	0.30	27.1				3.08	3.3						
	0.60	12.8				6.18							
	0.90	-1.6				9.26							
	1.20	-15.9				12.34							
	1.50	-30.2				15.45							
	1.76	-41.4				17.85							

appears, therefore, that turbulence in the water boundary layer caused oil to become entrained in the water. The occurrence of Kelvin-Helmholtz waves at the interface could not be verified.

From the mathematical model, a diesel fuel recovery rate of 13.5 L/min was predicted at a test facility drum rotation of 5 rpm. This was within 16 percent of the 11.6 L/min recovery rate measured in the flume. As the drum speed was increased, turbulence set in and the oil film suffered losses by entrainment. The predicted oil recovery rate became considerably greater than the observed one.

The decrease in the calculated diesel oil layer thickness on the experimental drum with an increasing drum speed indicated that there had been an insufficient oil supply to satisfy the maximum recovery rate of which the test facility was capable (see Figure 8). This also contributed to the increasing disparity between the theoretical and the experimental recovery rates, shown in Table 4 as the drum speed increased. The agreement of predicted and experimental results at the low drum speeds indicated that the collection process under laminar conditions was conducive to mathematical modelling.

The predicted oil recovery rate of 83.0 L/min for Oil Mix No. 54 was nearly five times the experimentally observed rate even at low rpm. This was largely due to the inadequate supply of Oil Mix No. 54 introduced to the flume during the tests. The capacity of the drum to recover the oil exceeded the supply rate.

7 GUIDELINES FOR OPERATION OF OSCAR

Experimental and mathematical studies show that pumping of the surface fluid does not play a significant role in determining the oil recovery rate of contra-rotating drums. Mathematical studies indicate that optimum recovery rates with minimum emulsification of oil in water would be achieved by the drum, if the Reynolds number of the water boundary layer which formed outside the drum oil film, was kept below 5×10^5. The mathematical studies also indicate that if there were an adequate oil layer thickness in front of the drum to supply the recovery demand, then increasing the drum speed would result in an increase in the oil layer thickness picked up by the drum.

The following guidelines for the operation of the prototype OSCAR have been drawn from these conclusions, and from the experimental observations:

1. The gap distance between the drums is not critical to the collection process; but it should be maintained sufficiently wide so that contact between the oil films on either drum does not occur. A gap width of 1 cm or more would be adequate for use in most light and medium oils.
2. The greatest effect of drum submergence is to increase the wetted perimeter of the drum which causes reduction of the maximum speed at which the drum can rotate without developing a turbulent boundary layer. Any existing wave action would both "wash" the oil layer on the drum and continuously change the length of wetted perimeter. In small waves, a drum submergence of 36 cm or greater, giving drum entry and exit angles to the water surface of 45 degrees or more, would minimize the worst wave effects. In calm waters the submergence may be reduced with a corresponding increase in drum speed and recovery rate.
3. The drums should be rotated at speeds of about 5 rpm when operating in thin oil slicks or with a drum submergence greater than 30 cm. This minimizes emulsification and the escape of oil droplets past the drums. The drum speed which would achieve the maximum recovery rate without regard for Oil Recovery Factor was not established, but this may be as high as 30 rpm for light oils. At this rotational speed, a drum submergence of less than 4 cm would be required to maintain a Reynolds number below 5×10^5 in the water boundary layer when there is a slick thickness greater than 1 cm.

4. The vessel pushing speed should be suited to the thickness of the oil slick. A speed of less than 0.2 m/s is recommended for oil spills where the thickness is greater than 1 cm. This will minimize the buildup of oil between the drums and reduce the amount of drainage failure, or oil which passes underneath the vessel. For oil spills with a thickness of less than 1 cm, the vessel speed should be increased sufficiently so that a localized layer buildup will develop in front of the forward drum and a continuous adequate supply will be available for collection.

Operation of the prototype OSCAR has indicated that installation of a downstream surface barrier to contain oil which has passed out from under the drums is a requisite for satisfactory operation. The test observations confirmed the need for such a downstream barrier. The barrier could be an integral component of the skimmer. Consideration should also be given to introducing a pump suction hose into the oil/emulsion buildup between the collecting drums and of pumping the emulsion into the collecting hulls when operating in light oils. An alternative system may be to scrape the water boundary layer from the rearward drum and to "wick" the emulsified oil onto the rearward drum through matting or by a foam roller.

REFERENCES

Milgram, J.H. and R.J. Van Houten, "Mechanics of a Restrained Layer of Floating Oil above a Water Current", J. Hydronautics, 12 (3), (July 1978).

Morris Industries, Private Communication.

Rosenhead, L. Laminar Boundary Layers, Oxford at Clarendon Press, (1963).

Schlichting, H. Boundary Layer Theory, McGraw-Hill, New York, (1955).

Solsberg, L.B., et al. , "Field Evaluation of Seven Oil Spill Recovery Devices", Environmental Protection Service, Environment Canada Report No. EPS4-EC-76-3, (August 1976).

Tallmadge, J.A., and C. Gutfinger, "Entrainment of Liquid Films - Drainage, Withdrawal and Removal", J. Industrial and Engineering Chemistry, 5p (11), (November 1967).

Unno, H. and Inoue, I. "Initial Behaviour of Oil Slicks", J. Chem. Eng. of Japan, 11(1), (1978).

APPENDIX I

ENTRAINMENT OF LIQUID FILMS

APPENDIX I ENTRAINMENT OF LIQUID FILMS

Knowledge of the dynamics of liquid films on solid objects is important in diverse fields such as coating, draining and lubrication. Tallmadge and Gutfinger (1967) summarized existing theories and proposed simplified design equations for the processes of withdrawal, removal and drainage.

The predominant forces in these processes are viscous, gravitational and interfacial surface tension. Inertial or acceleration forces may also be significant.

Withdrawal:

If a liquid film is considered on a vertical plate which is being withdrawn from a liquid bath, the Navier-Stokes equations for a constant flux and constant film thickness reduce to:

$$\mu \frac{d^2u}{dy^2} - \rho g = 0 \tag{1}$$

where the z coordinate is in the direction of the plate and y is in the direction perpendicular to the plate. If it is assumed that there is no slip at the plate boundary and no shear at the liquid/air interface, the following velocity profile is obtained:

$$\frac{u}{U} = 1 - \frac{\rho g h_o{}^2}{2\mu U}\left(\frac{y}{h_o}\right)\left(2 - \frac{y}{h_o}\right) \tag{2}$$

where

u = liquid velocity in the film;

U = plate velocity;

ρ = density of liquid;

g = gravitational constant;

μ = viscosity of liquid; and

h_o = constant film thickness.

The flux is obtained by integrating over the film thickness:

$$\frac{q}{U} = \int_o^{h_o} \frac{u}{U} = h_o \frac{\rho g h_o{}^3}{3\mu U} \tag{3}$$

In withdrawal, the flux is not specified and an estimate of the film thickness is necessary to determine the flux in constant flux withdrawal. It has been found that good agreement with experimental results is obtained if the film thickness is determined using a static meniscus boundary condition. This leads to the low speed and gravity corrected theories of withdrawal; the latter is the most general of the solutions.

The approach is based on an arbitrary division of the liquid film into three regions:

1. the constant thickness region above the liquid bath;
2. the dynamic portion of the meniscus adjoining liquid film;
3. the static portion of the meniscus near the free surface.

The assumptions made were:

a. the curvatures of the menisci of regions 2 and 3 were matched.
b. the miniscus in region 3 was assumed to be static (negligible viscous term).
c. the miniscus in region 2 was determined using one dimensional flow, no effect of flow on change in interfacial pressure and negligible film thickness gradient.

By these assumptions the Navier-Stokes equations in region 2 reduces to:

$$\sigma \frac{d^3h}{dz^3} + \frac{\mu d^2u}{dy^2} - \rho g = 0 \qquad (4)$$

where σ = surface tension, measured as force per unit length. This equation was solved for curvature and matched to the curvature of the static meniscus to yield the following thickness:

$$h_o \left(\frac{\rho g}{\sigma}\right)^{0.5} = 0.944 \left(\frac{\mu U}{\sigma}\right)^{0.66} \left[1 - \frac{h_o^2 \rho g}{\mu U}\right]^{0.66} \qquad (5)$$

Equation (5) is termed the gravity corrected theory of withdrawal.

If equation (5) is written in terms of the following two dimensionless numbers:

$$\frac{\text{viscous force}}{\text{surface tension}} = C_a = \frac{\mu U}{\sigma} \qquad \text{(capillary number)}$$

$$\frac{\text{gravitational force}}{\text{viscous force}} = T_o = h_o\left(\frac{\rho g}{\mu U}\right)^{0.5}$$

there results:

(6) $$\frac{T_o}{\left[1-T_o^{\,2}\right]^{0.67}} = 0.944\ C_a^{\ 0.17}$$

Drainage:

Upon removal of an object from a liquid bath, free drainage can be assumed to start. If it is assumed that the flow is so slow that only viscous and gravitational forces are significant, the flux of the liquid film can be shown to be:

$$q = \frac{\rho g h^3}{\mu} \qquad (7)$$

the continuity equation for the film is:

$$\frac{\partial q}{\partial z} = -\frac{\partial h}{\partial t} \qquad (8)$$

These equations together with the upper boundary condition of zero film thickness (h = o at z = o) result in the free drainage prediction:

$$h^2 = \frac{\mu z}{\rho g t} \qquad (9)$$

Inclusion of the acceleration term $\rho \frac{\partial u}{\partial t}$ in the equation of motion for the free drainage theory results in improvements of less than 1 percent.

APPENDIX II

OIL BOUNDARY LAYER THEORY

APPENDIX II OIL BOUNDARY LAYER THEORY

A steady state force balance can be written on the elemental volume of fluid in the oil boundary layer of the upstream drum (see Figure 9). The forces per unit width are:

$$P\,dy - \left(P + \frac{\partial P}{\partial s}ds\right) dy + \tau ds - \left(\tau + \frac{\partial \tau}{\partial y}dy\right) ds - g\left(\rho_\omega - \rho_o\right) dy\, ds \sin\theta = 0$$

where: P = static pressure;

s = distance from start of water boundary layer;

τ = shear force;

ρ_o = density of oil; and

ρ_ω = density of water;

(other symbols are as defined on Figure 9).

Let $\Delta\rho = \rho_\omega - \rho_o$, then the above equation can be simplified to:

$$\frac{\partial \tau}{\partial y} = \frac{\partial P}{\partial s} - g\,\Delta\rho \sin\Theta \qquad (1)$$

If the pressure gradient $\frac{\partial P}{\partial s}$ is determined from the flow outside the boundary layer, its magnitude is primarily dependent on the hydrostatic head, since in the free stream flow the horizontal pressure gradient is assumed to be zero.

Hence $$\frac{\partial P}{\partial s} = \frac{dP}{ds} = \frac{dP}{dy} = \frac{dy}{ds} = \gamma \sin\Theta$$

Substitution into equation (1) leads to :

$$\frac{\partial \tau}{\partial y} = -g \sin\Theta\,(\rho + \Delta\rho) \qquad (2)$$

Integration from the drum surface over a thickness y of the oil film yields:

$$\int_{\tau=\tau_o}^{\tau} d\tau = \int_{y=o}^{y} -g\sin\Theta\,(\rho+\Delta\rho)\,dy \qquad (3)$$

$$\tau = \tau_o - yg\sin\Theta\,(\rho + \Delta\rho)$$

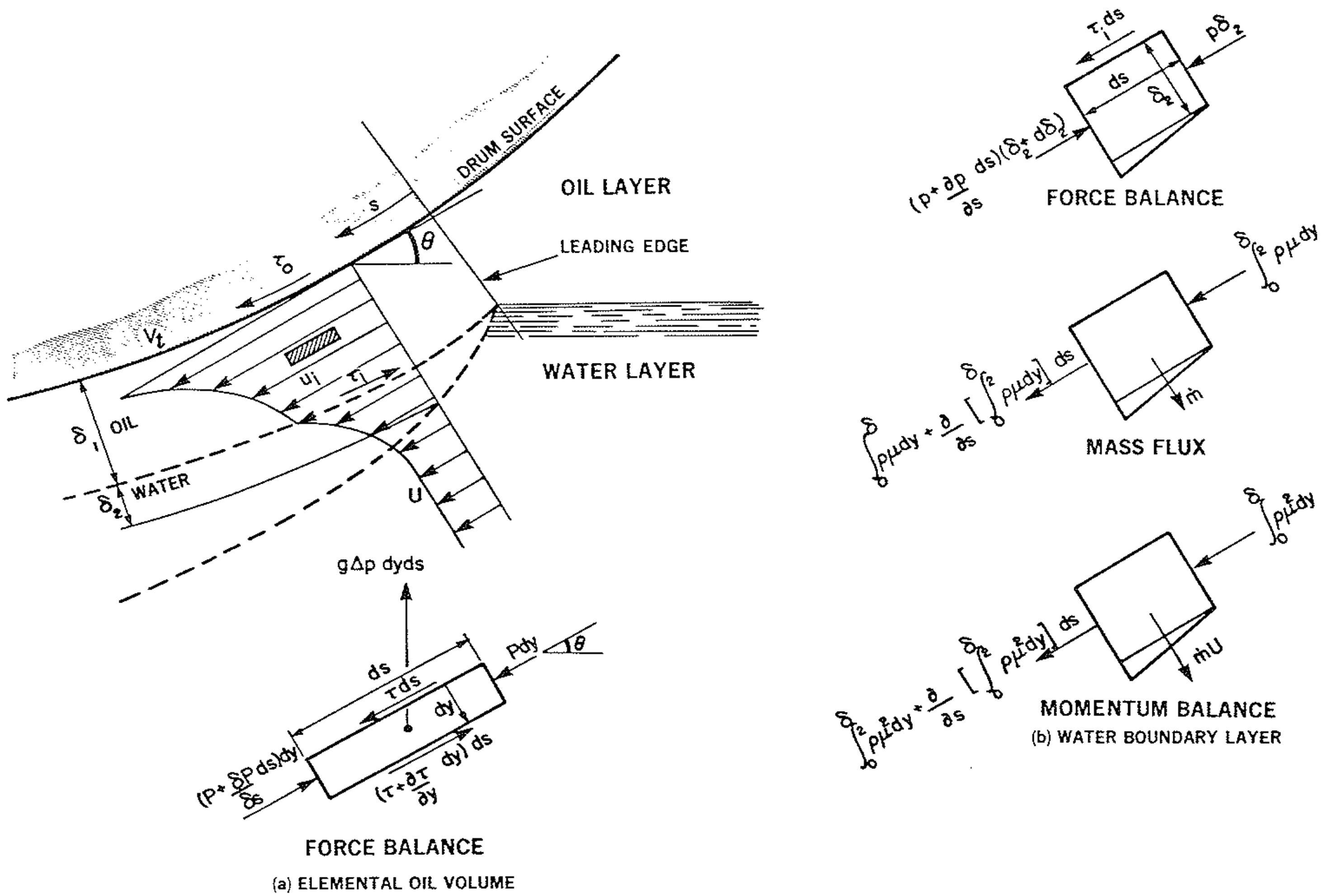

FIGURE 9 DEFINITION SKETCH FOR FORCE AND MASS BALANCE PER UNIT WIDTH

At the oil/water interface, $y = \delta_1$, the value of the shear stress is $\tau = \tau_i$:

$$\tau_i = \tau_o - \delta_1 g \sin \Theta (\rho + \Delta\rho) \qquad (4)$$

Since the velocity gradient in the oil can be expressed in terms of the oil shear stress:

$\frac{du}{} = \frac{-\tau}{}$, it follows that

$$\frac{du}{dy} = \frac{-\tau_o}{\mu} + \frac{yg \sin \Theta (\rho + \Delta\rho)}{\mu}$$

This equation can be integrated to find the velocity in terms of τ_o and y:

$$\frac{du}{dy} = V_t - \frac{\tau_o y}{\mu} + \frac{gy^2 \sin \Theta (\rho + \Delta\rho)}{2\mu} \qquad (5)$$

where V_t = drum surface velocity

The discharge of oil in the boundary layer is :

$$q = \int_{y=o}^{\delta^1} \mu dy = V_t \delta_1 - \frac{\tau_o \delta_1^2}{2\mu} + \frac{g\delta_1^3 \sin \Theta (\rho + \Delta\rho)}{3\mu} \qquad (6)$$

The Reynolds number is used as a criterion for the onset of turbulence in the boundary layer. It is usually evaluated in terms of the free stream velocity and the distance from the leading edge.

$$R_s = \frac{sU_e}{n} \qquad (7)$$

where:

s = distance along the boundary layer from the leading edge;

ν = kinematic viscosity of the oil;

$U_e = u_i - U$ = effective free stream velocity;

u_i = velocity at oil/water interface; and

U = free stream velocity outside of the water boundary layer.

Turbulence generally sets in when R_s exceeds a value of approximately 5×10^5.

APPENDIX III

WATER BOUNDARY LAYER

APPENDIX III APPLICATION OF VON KARMAN MOMENTUM - INTEGRAL EQUATION TO WATER BOUNDARY LAYER

It is assumed that the leading edge of the water boundary layer corresponds with the cooridinate s = o (see Figure 9a). It is further assumed that the flow is steady and two-dimensional. For the application of the Von Karman momentum - integral equation, the oil/water interface may be considered as one boundary for the water boundary layer. Consider a control volume consisting of an element of the water boundary layer with length ds, (see Figure 9b). The forces on the element in the "s" direction consist of the shear force, τ_i ds, at the oil/water interface and the pressure forces at each end of the control volume. The net force is:

$$F_s = \rho\delta_2 - \left(\rho + \frac{\partial \rho}{\partial s} ds\right)\left(\delta_2 + d\delta_2\right) + \tau_i \, ds$$

Upon simplifying, noting that $\frac{\partial p}{\partial s} = \gamma \sin \Theta$ and neglecting second order terms the net "s" force reduces to:

$$F_s = \left(\tau_i + \delta_2 \, \gamma \sin \theta\right) ds$$

The mass flux "$\dot{m}$" out of the control volume is equal to the mass flux in less the mass flux out. Similarly, the momentum flux U out of the control volume is equal to the momentum flux in, less the momentum flux out.

The mass flux $\dot{m}$ equals:

$$\dot{m} = \int_o^{\delta_2} \rho u dy - \left[\int_o^{\delta_2} \rho u dy + \frac{\partial}{\partial s} \int_o^{\partial_2} \rho u dy \; ds\right]$$

$$\dot{m} = - \frac{\partial}{\partial s} \left(\int_o^{\delta_2} \rho u dy \right) ds$$

so that the "s" momentum flux of the fluid crossing the bottom surface is:

$$\dot{m} U_e = - U_e \frac{\partial}{\partial s} \left(\int_o^{\delta_2} \rho u dy \right) ds$$

The totals "s" momentum flux out of the control volume is:

$$\int_0^{\delta_2} \rho u^2 dy + \frac{\partial}{\partial s}\left(\int_0^{\delta_2} \rho u^2 dy\right) ds - \int_0^{\delta_2} \rho u^2 dy - U_e \frac{\partial}{\partial s} \int_0^{\delta_2} \rho u dy \; ds$$

simplifying and noting that:

$$U_e \frac{\partial}{\partial s}\left(\int_0^{\delta_2} \rho u dy\right) = \frac{\partial}{\partial s}\left(\int_0^{\delta_2} \rho u U_e dy\right) - \frac{\partial U_e}{\partial s} \int_0^{\delta_2} \rho u dy$$

the total "s" momentum flux out of the control volume is:

$$\frac{\partial}{\partial s} \int_0^{\delta_2} \rho u\left(\left(u - U_e\right) dy\right) ds + \frac{\partial U_e}{\partial s} \int_0^{\delta_2} \rho u dy \; ds$$

The surface forces in the "s" direction are now equated with the total "s" momentum flux out of the control volume. It is assumed that the free stream velocity U_e equals $U - u_i$. This implies that the free stream velocity U is always parallel to the boundary layer which is not strictly the case. The momentum integral equation then is:

$$\tau_i + \delta_2 \gamma \sin\theta = \frac{\partial}{\partial s}\left\{\int_0^{\delta_2} \rho u\left(u - \left(U - u_i\right)\right) dy\right\} + \frac{\partial}{\partial s}\left(U - u_i\right) \int_0^{\delta_2} \rho u dy$$

Approximate Solution of Water Boundary Layer

In the approximate solution of the water boundary layer use was made of the momentum integral equation, part A, and the approximate solution methods described in chapter 12 of Schlichting, (1955).

As the free stream velocity U is numerically smaller than u_i, the quantity (U-u) is negative. The effective free stream velocity is defined as:

$$-U_e = U - u_i$$

The momentum integral equation then is:

$$\tau_i + \delta_2 \gamma \sin\theta = \frac{d}{ds}\int_o^{\delta_2} \rho u \left(u + U_e\right) dy - \frac{dU_e}{ds}\int_o^{\delta_2} \rho u dy \qquad (1)$$

Introducing the momentum thickness "m":

$$mU_e^2 = \int_o^{\delta_2} u \left(u + U_e\right) dy \qquad (2)$$

Substitution into equation (1) yields:

$$\tau_i + \delta_2 \gamma \sin\theta = \rho \frac{d}{ds} \left(mU_e^2\right) - \frac{d}{ds} U_e \int_o^{\delta_2} \rho u dy \;\; ds \qquad (3)$$

It is assumed that the interfacial and free stream velocities change slowly with distance, so that $\frac{d}{ds}(U_e) = o$

Equation (3) simplifies to:

$$\tau_i + \delta_2 \gamma \sin\theta = \rho U_e^2 \frac{dm}{ds} \qquad (4)$$

A reasonable velocity profile is now introduced for the water boundary layer:

$$\frac{\mu}{-U_e} = 1 - f\ (y/\delta_2) = 1 - f\ (n) \qquad (5)$$

where $n = y/\delta_2$ and $\delta_2\, dn = dy$

Evaluation of the integral of equation (2)

$$\int_o^{\delta_2} u\,(U + U_e)\ dy$$

in terms of the velocity distribution of equation (5) leads to

$$- \int_o^1 \delta_2\, U_e^2 f\,(1 - f)\ dn$$

let $$I = -\int_0^1 f(1-f)\, dn$$

so that $$m = I\ \delta_2 \qquad (6)$$

Introducing the displacement thickness δ^*:

$$\delta^* (U - u_i) = \int_0^{\delta_2} u - (U - u_i)\ dy$$

$$-\delta^* U_e = \int_0^{\delta_2} (u + U_e)\ dy$$

$$\delta^* U_e = -\int_0^1 \delta_2\, U_e\, f\ dn$$

Let $$2 = -\int_0^1 f\ dn$$

then $$\delta^* = 2\ \delta_2 \qquad (7)$$

The interfacial shear can be represented by the relationship:

$$-\frac{\tau_i}{\rho} = \nu_2 \frac{du}{dy}\Bigg|_{y=o} = \nu_2 (-U_e) \left(-\frac{\partial f}{\partial n}\frac{\partial n}{\partial y}\right)$$

where $\frac{\partial f}{\partial n} = f^1(0) = \beta_1$, and $\frac{\partial n}{\partial y} = \frac{1}{\delta_2}$, leading to the

relationship:

$$\frac{\tau_i}{\rho} = \frac{\nu_2\ U_e}{\delta_2}\ \beta_1 \qquad (8)$$

Substitution of the value of τ_i of equation (7) and the value of m of equation (6) into equation (4) results in:

$$\delta_2 \frac{d\delta_2}{ds} = \frac{\nu_2 \beta_1}{\alpha_1 U_e} + \frac{\delta_2^2 \, y \sin\vartheta}{\rho U_e^2 \alpha_1} \tag{9}$$

An approximate solution to this equation can be obtained by neglecting the last term, which represents the pressure gradient, and integrating from $\delta_2 = 0$ at $s = 0$:

$$\delta_2 = \left(\frac{2\beta_1}{\alpha_1} \cdot \frac{\nu_2 S}{U_e} \right)^{0.5} \tag{10}$$

the interfacial shear from equation (4) then becomes:

$$\tau_i = \left(\frac{\alpha_1 \beta_1}{2} \right)^{0.5} \mu_2 U_e \left(\frac{U_e}{\nu_2 S} \right)^{0.5} \tag{11}$$

Both the water boundary layer thickness and the interfacial shear can now be evaluated as a function of distance from the leading edge, the effective free stream velocity and the fluid viscosity. As the oil film thickness is small, the interfacial velocity will be nearly that of the surface of the drum so that the effective free stream velocity can be assumed to be:

$$-U_e = U - V_t$$

Determination of the interfacial shear, τ_i, permits the velocity distribution and the discharge of the oil film to be calculated by the use of equations (6) and (7) of section 8.